

Fermi National Accelerator Laboratory

FERMILAB-TM-1986

Simple Model of Calorimeter Sampling Response in a Magnetic Field

Dan Green

*Fermi National Accelerator Laboratory
P.O. Box 500, Batavia, Illinois 60510*

October 1996



Disclaimer

This report was prepared as an account of work sponsored by an agency of the United States Government. Neither the United States Government nor any agency thereof, nor any of their employees, makes any warranty, express or implied, or assumes any legal liability or responsibility for the accuracy, completeness or usefulness of any information, apparatus, product or process disclosed, or represents that its use would not infringe privately owned rights. Reference herein to any specific commercial product, process or service by trade name, trademark, manufacturer or otherwise, does not necessarily constitute or imply its endorsement, recommendation or favoring by the United States Government or any agency thereof. The views and opinions of authors expressed herein do not necessarily state or reflect those of the United States Government or any agency thereof.

Distribution

Approved for public release: further dissemination unlimited.



Simple Model of Calorimeter Sampling Response in a Magnetic Field

Dan Green
Fermilab

Introduction:

The fact that plastic scintillator "brightens" in the presence of a magnetic field has been known for some time. Recently, measurements have been extended to larger field strengths (< 20 T) and a saturation of the effect was observed for fields > 2.5 T. Thus the active element in a sampling calorimeter may be expected to have a signal increase of $\sim 6-8\%$ when immersed in fields of strength > 2.5 T. [1] This brightening of the scintillator is independent of the orientation of the field.

In addition to these effects, there has been reported an increase in the signal seen by sampling calorimeters due to incident electrons in the presence of a magnetic field. [2] In contrast to the brightening effect, there does not appear to be saturation at the field strengths used ($B < 2.5$ T) and the magnitude of the effect appears to be somewhat larger than that expected from brightening alone, $\sim 20\%$ at 2.5 T. A comprehensive program has been mounted to study these problems in the context of CMS calorimetry and new results are expected momentarily. [3] In particular, field strengths up to 3 T are employed, and field orientations parallel and perpendicular to the incident particle are to be explored.

Simplified Model:

In addition, GEANT based Monte Carlo studies have been begun in order to have a model of the data. [4] Nevertheless, although such models can be considered to be complete, a simple model which is more transparent is often a useful adjunct to full GEANT investigations. For this reason, a simple model which attempts to extract the essential physics was written to be compared to the GEANT results and to preliminary CMS HCAL data from test beam work.

The model begins with electrons emerging from an Cu absorber plate. Photons are ignored, although they do, indeed, transport a substantial fraction of the energy of an electromagnetic cascade. The critical energy in Cu is about 20 MeV, while that in scintillator is about 70 MeV. Thus the emerging electrons will lose energy by nonradiative processes in the active plastic of the sampling calorimeter. Specifically, electrons were chosen from a power law distribution from a cutoff energy (0.1 MeV) up to the plastic scintillator critical energy, 20 MeV. Note that simple models have the advantage of running fast even when the cutoff is lowered, thus perhaps exposing physics avoided in the interest of computational time. One variable of the model is the power a , where the electron kinetic energy T_e is distributed as $1/T_e^a$. The magnitude of a is indicated by classical shower theory to be, $a \sim 0.5$. [5]

The e direction is taken to be normal to the sampling plate plane, i.e. in the direction of the incident particle. Therefore, shower particle angles, in particular multiple scattering, are ignored. One could easily add an angular distribution to the model, but this has not yet been explored.

Given the e exiting the absorber plate, one propagates in a uniform field by a perpendicular distance l to the entrance of the scintillator plate. The second step is to the exit plane of the scintillator, taken to have a thickness d . Multiple scattering is ignored, as is energy loss, in evaluating the e trajectory. Electrons which loop in the field are properly taken account of. There are 3 cases; 1 - electron loops in step to l , no energy deposit in active layer, 2 - electron loops in step to d , path length in scintillator is from entrance at $z = l$ to exit at $z = l$ (z along the incident particle trajectory), 3 - electron traverses scintillator to $z = l + d$, path length in scintillator is from entrance at $z = l$ to exit at $z = l + d$. The geometry for the 3 cases is shown in Fig.1.

The path length in the active scintillator is then known. The path length for a 40 kG field strength, $l = 1$ mm, $d = 4$ mm is shown in Fig.2. The entries at 0 are due to the loopers of case 1. The peak at ~ 4 mm is due to e with small bend angles, while the tail at larger path lengths is due to the increased arc length in the presence of the field. The path length at zero field strength is 4 mm by assumption. The energy deposit is taken to be that of a minimum ionizing particle unless the electron ranges out. In the latter case, the full electron kinetic energy is taken to be deposited, T_e . Thus, we ignore the possibility of tuning the "cladding" layer l , assuming it is vacuum. That tuning is the purview of full GEANT. [6]

Model Results:

The mean kinetic energy follows from the power law exponent and the limits for populating T_e . For $a = 1/2$, $\langle T_e \rangle = 7$ MeV. In the case $l = 1$ mm, $d = 4$ mm, the energy deposit in the

scintillator is shown in Fig.3. In comparison, the energy deposit at 0 field for a minimum ionizing particle is ~ 0.6 MeV. The mean path length in Fig.2 is $\langle s_B \rangle = 5.34$ mm, or a 34% path length increase. The mean energy deposit at 40 kG is $\langle TB \rangle = 0.75$ MeV, compared to the result at zero field, $\langle T0 \rangle = 0.54$ MeV. The ratio of the energy deposit with respect to that at 0 field strength is plotted in Fig.3 for 10,20,30, and 40 kG. The effect of the loopers and the increased path length is clearly evident.

The power law controlling the distribution was adjusted to roughly agree with GEANT results. It was required to make $a \sim 1$, corresponding to $dNe \sim dTe/Te$. For the case $l = 0$ mm, $d = 4$ mm the ratio $\langle TB \rangle / \langle T0 \rangle$ is shown as a function of B_0 up to 3 T in Fig.4. A roughly linear increase of energy deposit with field strength is observed. Clearly, the path length will increase with B_0 , as the soft electrons are forced to curl up in tighter circles.

The "cladding" effect at $B_0 = 4$ T, and $d = 4$ mm was studied by measuring the energy deposit ratio, $\langle TB \rangle / \langle T0 \rangle$ as a function of l for $l = (0, 5 \text{ mm})$. The energy deposited in the 4 mm thick scintillator as a function of l at 40 kG is shown in Fig.5. Clearly, the fraction of loopers increases with field strength, as is seen in Fig.5. In addition, the e which reach the scintillator layer has a path length which increases with B_0 . The $\langle TB/T0 \rangle$ ratio is shown in Fig.6. As l increases, the ratio decreases as one is effectively increasing the cutoff energy for an e to reach the entrance scintillator plane. Therefore, one has the possibility, by properly "cladding" the scintillator, of tuning out the path length increase at a given field strength, B_0 , to zero by raising the "looper" cutoff energy to compensate for the increased path length. A fully quantitative study is properly done only in the GEANT context. Nevertheless, it appears that the main features of the effect are geometric rather than subtle differences in particle propagation in materials of varying Z and A .

References

1. D. Green, V. Hagopian, A. Rhonzin - Femilab TM-1937 (1995).
2. D. Blomker et al., NIM, A311, 505 (1992).
J. Manuisch et al., NIM, A312, 451 (1992)
3. Jim Freeman, private communication
4. Suichi Kunori, private communication
5. B. Rossi, High Energy Particles, Prentice Hall Inc. (1952)
6. F. Lemeilleur Et Al., Phys. Lett. B222, 518 (1989)

Figure Captions

- Figure 1. The geometry for this study showing the absorber exit plane, the space before the scintillator plate, and the plate itself. Also shown are e trajectories for the 3 possible cases discussed in the text.
- Figure 2. The distribution of path lengths in scintillator for $l = 1$ mm, $d = 4$ mm, $B_0 = 4$ T. The loopers at 0 length, the \sim straight e at 4 mm, and the increased path length for soft e are all evident.
- Figure 3. The energy deposit in the scintillator layer with respect to the energy deposit at 0 field strength. The loopers and increased path length effects are both evident, as is the peak for \sim straight line e trajectories.
- 10 kG
 - 20 kG
 - 30 kG
 - 40 kG
- Figure 4. The mean energy deposit in scintillator with respect to the $B_0 = 0$ T case for $l = 0$ mm, $d = 4$ mm as a function of B_0 . The mean increases with B_0 in a roughly linear fashion.
- Figure 5. The energy deposit in the 4 mm thick scintillator layer at $B_0 = 4$ T. E is in GeV units, and the peak at ~ 0.55 MeV due to \sim straight lines delivering minimum ionization is evident, as are the loopers and the increased path length of soft e in the magnetic field.
- $l = 0$ mm
 - $l = 1$ mm
 - $l = 2$ mm
 - $l = 3$ mm
- Figure 6. The mean energy deposit in scintillator with respect to the $B_0 = 0$ T case for $d = 4$ mm, $B_0 = 4$ T as a function of l . The power law is $dN_e \sim dT_e/T_e$. Note the 25% increase for no air gap and the \sim linear decrease of the effect with air gap, thickness l .

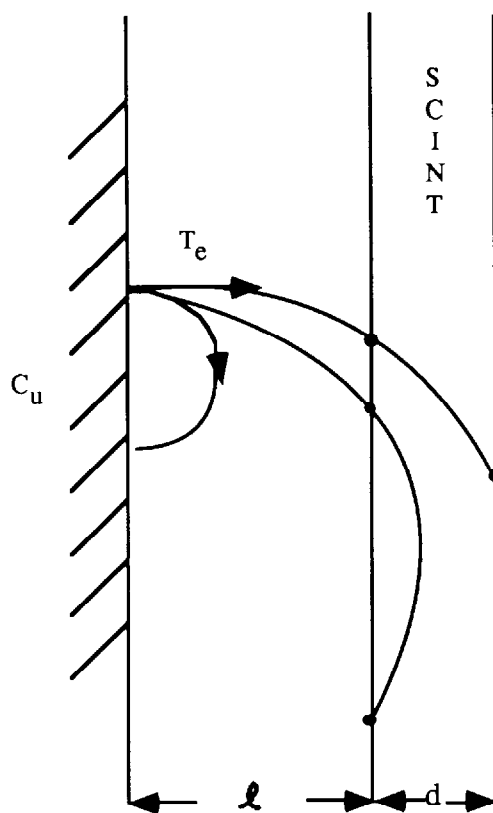


Figure 1

The geometry for this study showing the absorber exit plane, the space before the scintillator plate, and the plate itself. Also shown are e trajectories for the 3 possible cases discussed in the text.

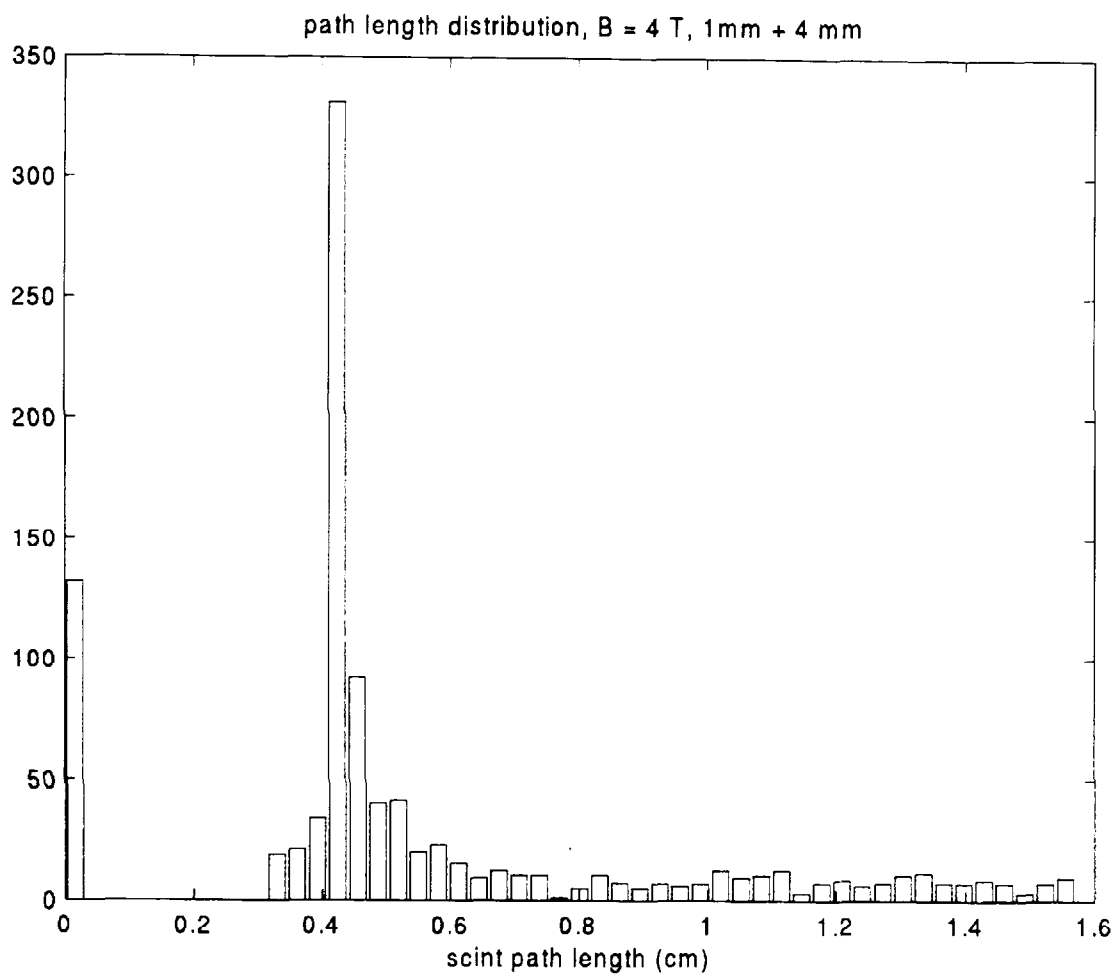


Figure 2

The distribution of path lengths in scintillator for $l = 1 \text{ mm}$, $d = 4 \text{ mm}$, $B_0 = 4 \text{ T}$. The loopers at 0 length, the \sim straight e at 4 mm, and the increased path length for soft e are all evident.

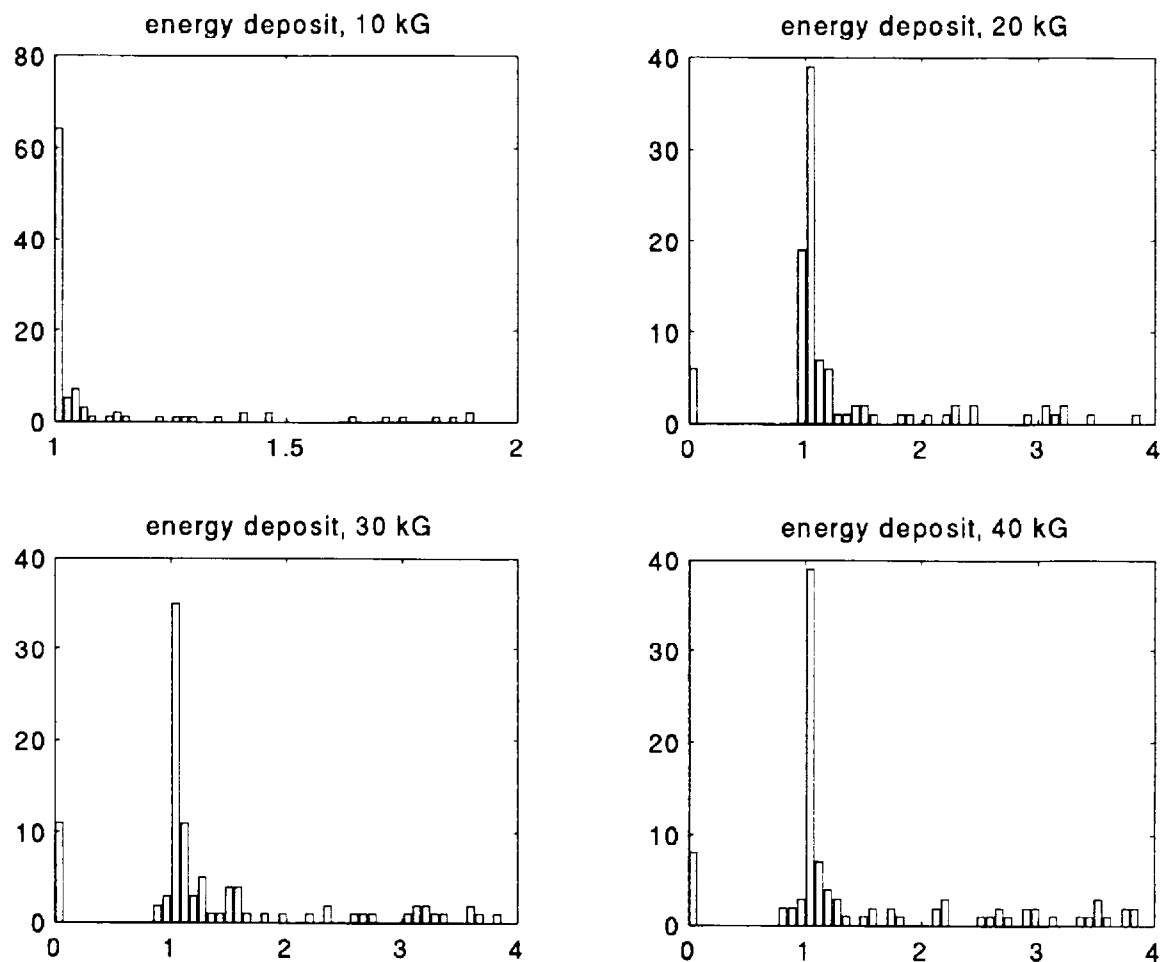


Figure 3

The energy deposit in the scintillator layer with respect to the energy deposit at 0 field strength. The loopers and increased path length effects are both evident, as is the peak for \sim straight line e^- trajectories.

- 10 kG
- 20 kG
- 30 kG
- 40 kG

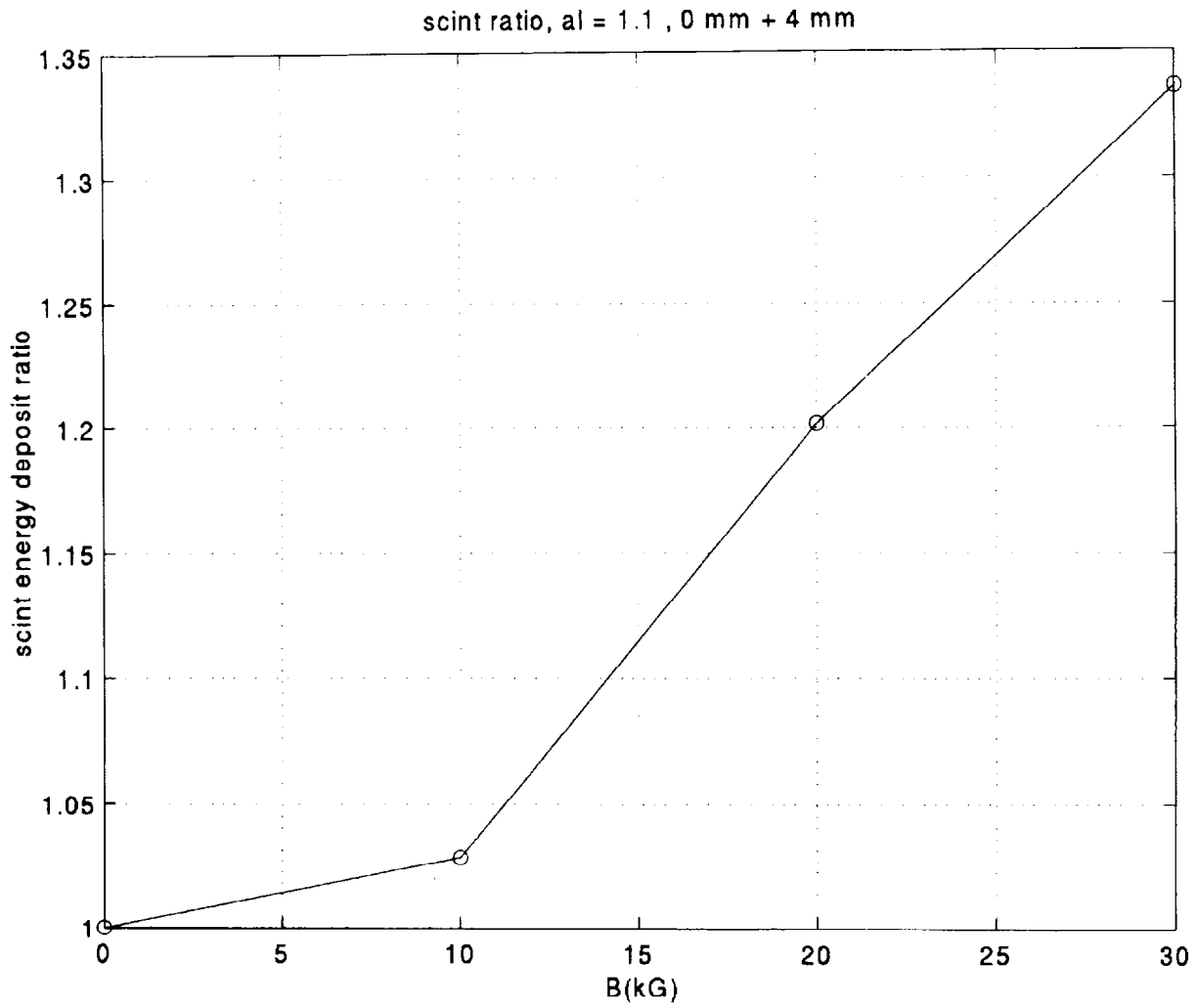


Figure 4

The mean energy deposit in scintillator with respect to the $B_0 = 0$ T case for $l = 0$ mm, $d = 4$ mm as a function of B_0 . The mean increases with B_0 in a roughly linear fashion.

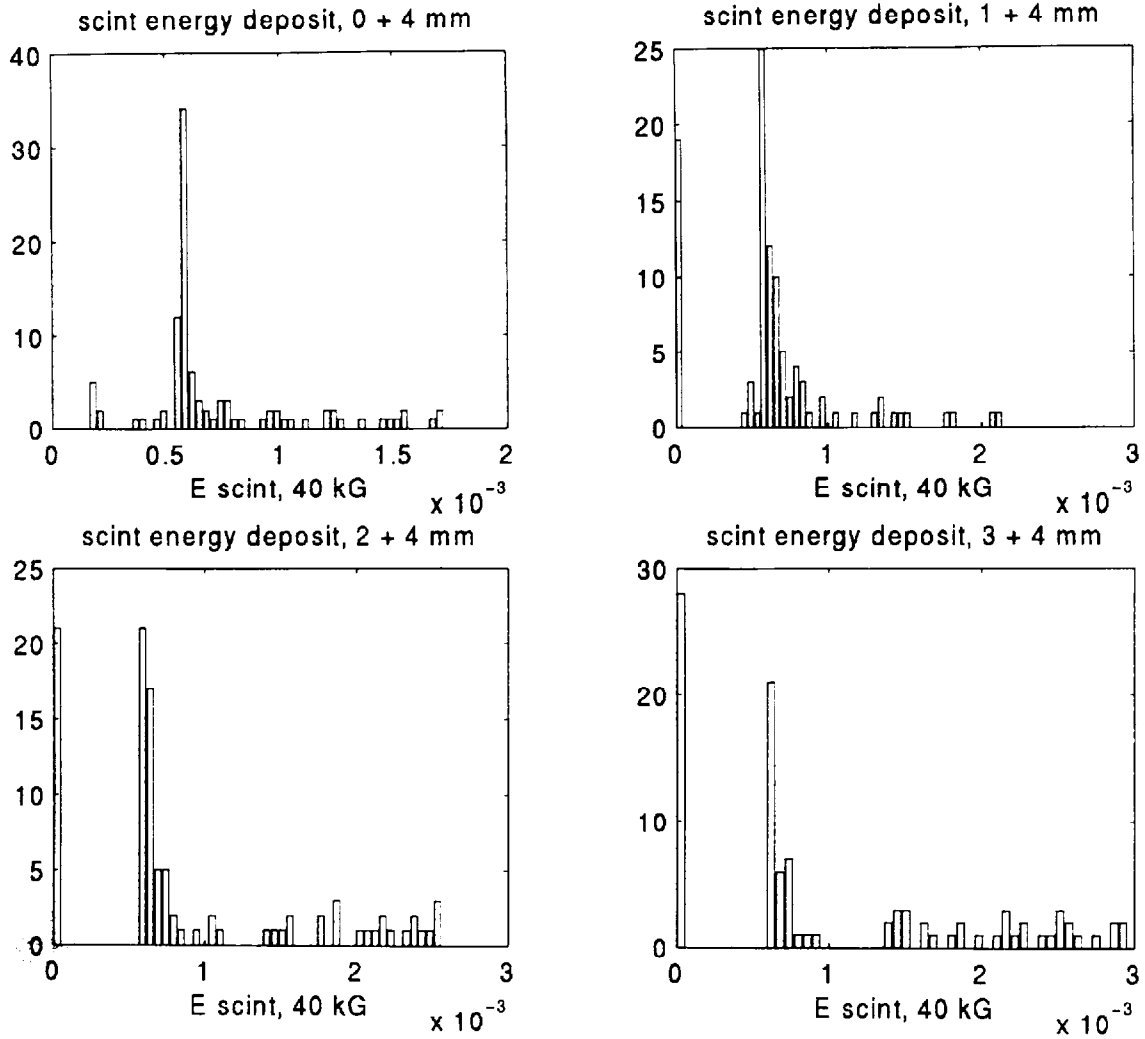


Figure 5

The energy deposit in the 4 mm thick scintillator layer at $B_0 = 4$ T. E is in GeV units, and the peak at ~ 0.55 MeV due to \sim straight lines delivering minimum ionization is evident, as are the loopers and the increased path length of soft e in the magnetic field.

- a. $l = 0$ mm
- b. $l = 1$ mm
- c. $l = 2$ mm
- d. $l = 3$ mm

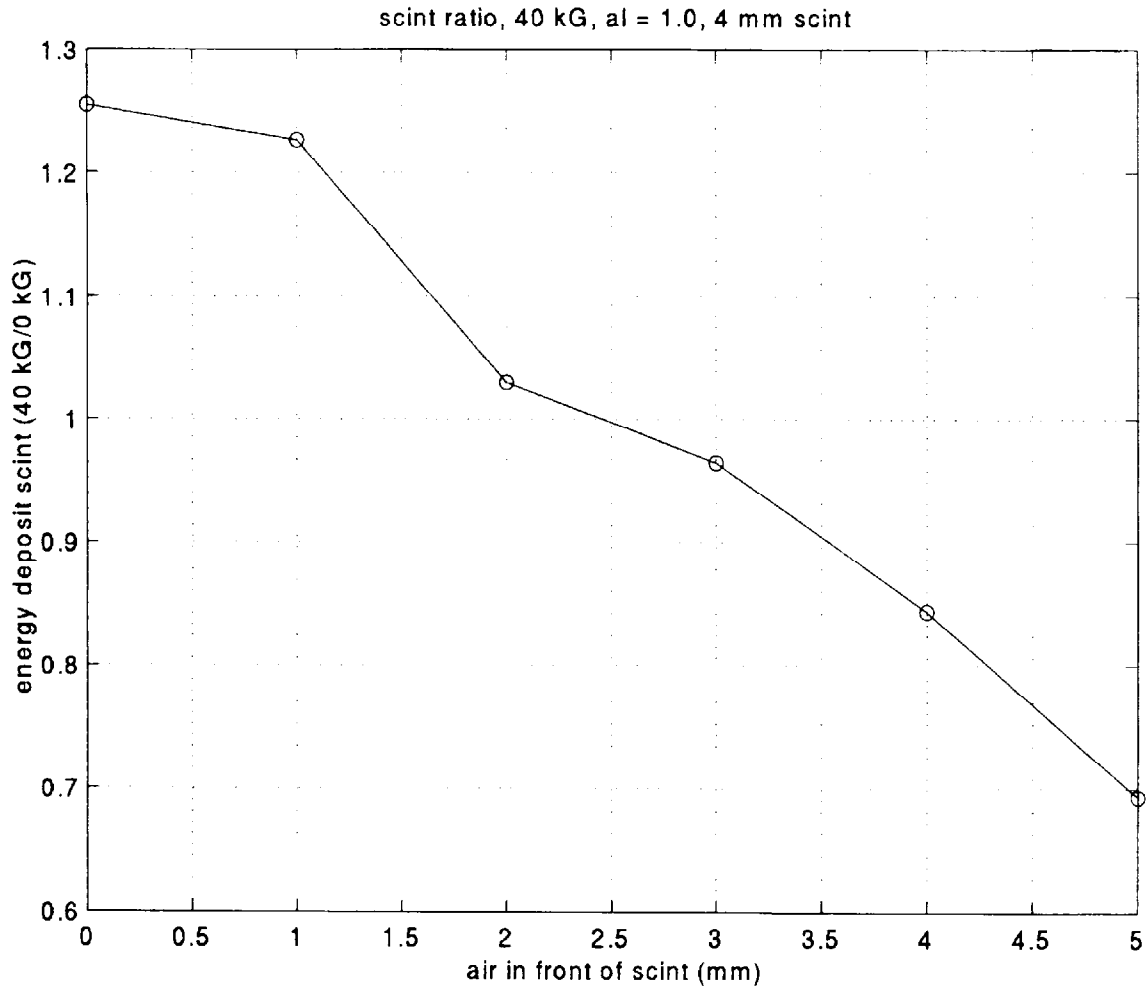


Figure 6

The mean energy deposit in scintillator with respect to the $B_0 = 0$ T case for $d = 4$ mm, $B_0 = 4$ T as a function of l . The power law is $dN_e \sim dT_e/T_e$. Note the 25% increase for no air gap and the \sim linear decrease of the effect with air gap, thickness l .